ORIGINAL PAPER

Albertas Malinauskas · Rudolf Holze

A UV-visible spectroelectrochemical study of the electropolymerisation of *N*-benzylaniline

Abstract The electropolymerisation of *N*-benzylaniline (NBA) at transparent ITO glass electrodes was investigated with in situ UV-visible spectroelectrochemistry. An intermediate was found to be generated during electrolysis as the precursor of poly(*N*-benzylaniline) (PNBA). The intermediate, which shows an absorbance band at $\lambda = 460$ nm, is able to react spontaneously with NBA, forming a polymeric end product, which is deposited on the electrode surface. UV-Vis spectra were obtained with PNBA-modified electrodes at various electrode potentials. It was shown that the colouration of the PNBA film after a positive-going potential step proceeds ca. 5 times slower than its discolouration after the reverse negative-going potential step. Anodic degradation of PNBA film was shown to proceed when holding the electrode at a sufficiently high positive potential. A linear dependence between the first-order degradation rate constant (k/s^{-1}) and electrode potential (E/V) was found in the potential range of $E_{RHE} = +0.8$ to $+1.1$ V: $\log k = a + bE$, where $a = -8.75$ and $b = 5.45$ are empirical coefficients. In the whole spectral range investigated, the degradation of PNBA was found to proceed faster as compared to that of polyaniline (for polyaniline, coefficients $a = -12.7$ and $b = 8.96$ were obtained in the potential range of $E_{RHE} = +0.85$ to $+1.1$ V). The electrooxidation of hydroquinone, as well as the electroreduction of benzoquinone, were shown to proceed at PNBA-modified electrodes. In these processes, PNBA was shown to play the role of an electron mediator between the ITO electrode and solution phase redox species.

A. Malinauskas[1] · R. Holze (✉)
Technische Universität Chemnitz, Institut für Chemie,
D-09107 Chemnitz, Germany
e-mail: rudolf.holze@chemie.tu-chemnitz.de

Permanent address:
[1] Institute of Chemistry, Gostauto Str. 9,
LT-2600 Vilnius, Lithuania

Introduction

Polyaniline derivatives are known to possess chemical and physical properties quite different from those characteristic of the parent polyaniline (PANI). Besides the fact that PANI is the only known intrinsically conducting polymer with nitrogen atoms being no part of an aromatic ring system and thus being available for protonation, PANI does not have a completely conjugated π-electron system in its reduced, poorly conducting state. The additional substituents of aniline derivatives are responsible for changed conductivity, chemical or electrochemical reactivity, stability versus environmental attack, etc. Most papers published so far on polyaniline derivatives refer to ring-substituted derivatives, whereas only scant attention has been paid to nitrogen-substituted ones. The introduction of a substituent, bound to the nitrogen atoms of PANI, obviously induces significant changes in the polymer structure, which may cause various differences in physicochemical properties. This enables the tailoring of intrinsically conducting polymer layers used as modifiers of electrodes for sensors, in electrocatalysis or as corrosion protection. A broad study of these influences will help in understanding the relationships between the structure of the monomer and polymer and the properties of the obtained polymer.

A great deal of attention focusing on *N*-substituted polyanilines was paid to the simplest of them, poly(*N*-methylaniline), whereas other derivatives were studied to a much lesser extent. Chiba et al. [1] obtained polymer films from *N*-methylaniline (NMA) and *N*-ethylaniline (NEA) by electropolymerisation in aqueous solution, which showed, in contrast to PANI, only one pair of anodic and cathodic peaks with an average potential of

$E_{SSCE} = 0.37$ V for both poly(N-methylaniline) (PNMA) and poly(N-ethylaniline) in 0.2 M perchlorate solution of pH = 1.0. In contrast, Barbero et al. [2] found for PNMA two pairs of anodic and cathodic voltammetric peaks, centred at $E_{SSCE} = -0.17$ V and 0.15 V in aqueous 1 M HClO$_4$, whereas PANI showed the corresponding redox processes at $E_{SSCE} = -0.30$ V and 0.25 V, respectively.

Comisso et al. [3] polymerised NMA both electrochemically and chemically and reported the electrical conductivity of PNMA to be 10^{-3} S/cm, i.e. lower than that of PANI but comparable to that of ring-substituted polyanilines, which suggests that probably similar structural distortions are introduced into the polymer backbone. A lower electric conductivity of PNMA as compared to PANI was reported also by other research groups. Langer [4] copolymerised NMA with aniline electrochemically, and pointed out a decrease of conductivity from about 10^{-1} to 10^{-6} S/cm with an increase of the content of PNMA in a copolymer from 0 to 100%. From IR spectra it was calculated that incorporation of NMA residues into the polyaniline structure is responsible for shorter polymer chains [4, 5].

A reversible anion exchange between the solution and PNMA can be assumed in the course of electrochemical redox processes. Barbero et al. [2] investigated an electrochemically synthesised PNMA film with probe beam deflection and a quartz crystal microbalance. They found anion insertion during anodic oxidation of PNMA and calculated an effective molar mass of the exchanged species of about 91 g/mol, which is in good agreement with the molar mass of the perchlorate ion of 99.5 g/mol, used in their experiments [2].

Except for PNMA, little information is available on other N-substituted polyanilines. Dao et al. [6, 7] obtained polymer films by electropolymerisation of a number of N-substituted anilines, including methyl, ethyl, benzyl, phenyl and naphthyl derivatives. For poly(N-phenylaniline), electropolymerised in acetonitrile solution, an unexpectedly high conductivity of 1 S/cm was reported, whereas poly(N-naphthylaniline) showed a conductivity of 10^{-3} S/cm [7]. Earlier, we reported electrochemical copolymerisation of N-(3-sulfopropyl)-aniline with NMA [8] and with aniline [9], leading to self-doped N-substituted PANI derivatives.

Unexpectedly, despite the lower electric conductivity, as compared to PANI, PNMA showed a more efficient electrocatalytic effect with the redox couple hydroquinone/benzoquinone [10, 11].

In the present study we have investigated the electropolymerisation of N-benzylaniline (NBA) at indium-doped tin oxide coated (ITO) glass electrodes and some properties of the obtained polymer with UV-vis spectroelectrochemistry. Previously, we studied with in situ UV-vis spectroelectrochemistry the electrooxidation of NMA [12].

Experimental

Electrolyte solutions were prepared from 18 MΩ water (Seralpur Pro 90C). As a supporting electrolyte, 0.5 M H$_2$SO$_4$ solution was used in all experiments.

UV-Vis spectra were recorded with a Shimadzu model UV-2101 PC spectrometer. Spectroelectrochemical experiments were done in a 1 cm path length quartz cuvette fitted with a transparent ITO glass working electrode with a specific surface resistance of 10–20 Ω/square, installed perpendicularly in the incident light path, a platinum wire counter electrode, and an auxiliary hydrogen reference electrode connected via a salt bridge. The reference electrode was filled with 0.5 M H$_2$SO$_4$ solution. Before experiments the ITO glass electrodes were degreased with acetone and rinsed with an excess of water. The reference channel of the spectrometer was occupied by a quartz cuvette containing an identical glass electrode. All spectra reported are background corrected.

A Wenking model LB 81 M laboratory potentiostat was used. All potential values given below refer to the relative hydrogen electrode, containing 0.5 M H$_2$SO$_4$.
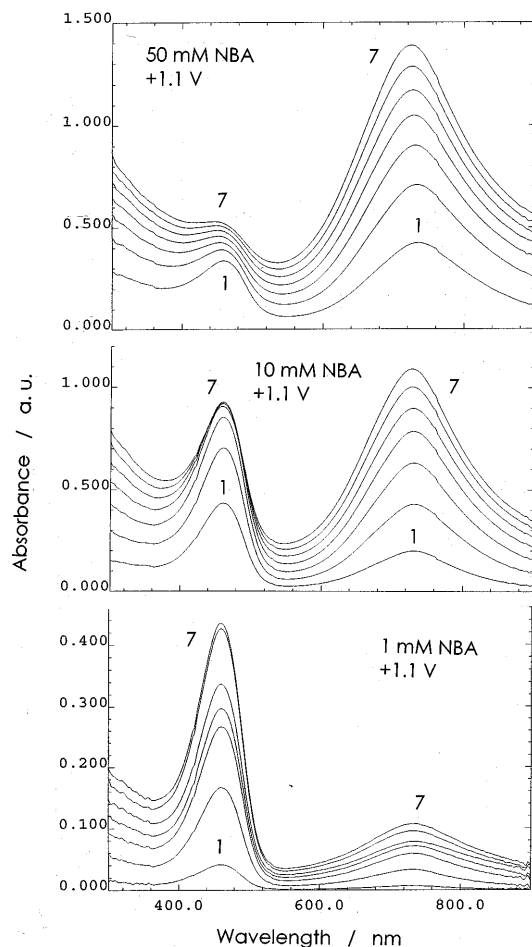
Results and discussion

Electropolymerisation of NBA

Figure 1 shows UV-vis spectra obtained after a positive-going electrode potential step from $E_{RHE} = 0$ V to $E_{RHE} = 1.1$ V with an ITO glass electrode in a solution of NBA. Two absorbance maxima located at $\lambda = 460$ nm and $\lambda = 730$ nm are well defined. Both maxima grow in height during continued electrolysis. The growth rate for both maxima depends on the NBA concentration in different ways. Figure 2 depicts absorbance transients for both maxima, obtained at the various concentrations of NBA used, ranging from 1 to 50 mM. It is seen that the growth rate of the absorbance band at $\lambda = 460$ nm increases with an increasing concentration of NBA up to ca. 5 or 10 mM. A further increase of NBA concentration beyond 10 mM causes a decrease of the initial growth rate of absorbance. It is also seen that the absorbance band at $\lambda = 460$ nm tends to saturate after 3 or 4 min of electrolysis, especially at higher concentration of NBA. In contrast, the growth rate of the absorbance band at $\lambda = 730$ nm increases with increasing concentration of NBA in the whole concentration range studied (Fig. 2).

After interruption of electrolysis the absorbance at $\lambda = 730$ nm continues to grow to some extent [Fig. 3 (top)], whereas the band at $\lambda = 460$ nm diminishes in height and disappears almost completely in a few minutes [Fig. 3 (bottom)].
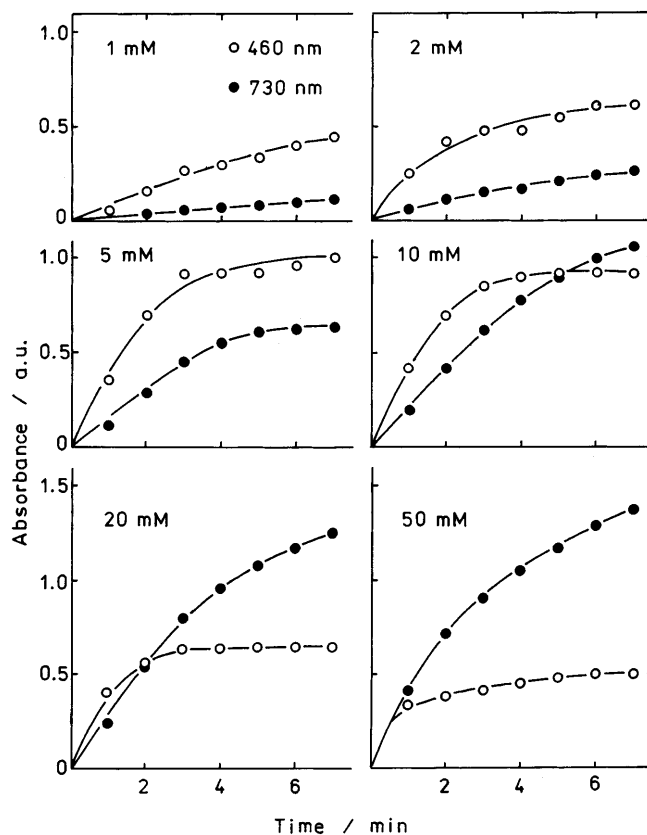
The tendencies observed (presented in Figs. 1, 2 and 3) can be interpreted in the framework of a two-step mechanism of electrooxidation of NBA. After applying a sufficiently high positive potential, electrooxidation of NBA proceeds leading to a reaction intermediate. This intermediate shows an absorbance band at $\lambda = 460$ nm. In the next following chemical step the intermediate

Fig. 3 Absorbance-time profiles recorded at $\lambda = 730$ nm (top) and $\lambda = 460$ nm (bottom) obtained after a potential step to $E_{RHE} = +1.1$ V, and after interruption of electrolysis (as indicated by the *arrows*, designed "on" and "off", respectively), in solutions containing different concentrations of NBA (as indicated)
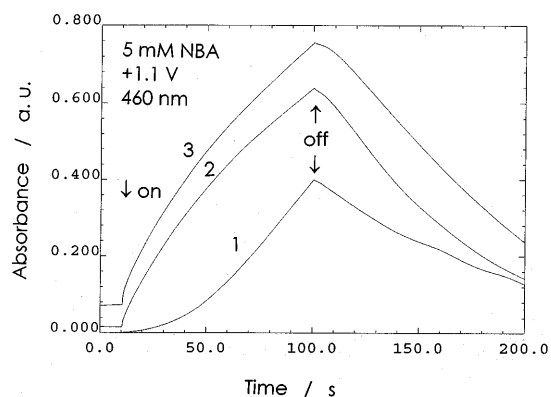
Fig. 4 Same as in Fig. 3 but recorded at $\lambda = 460$ nm in a solution of 5 mM NBA for the first, second and third time (as indicated)

PNBA film obtained at different electrode potential values ranging from $E_{RHE} = 0.2$ to 0.8 V. Spectra obtained at a potential of $E_{RHE} = 0.2$ and 0.3 V correspond to the reduced (leucoemeral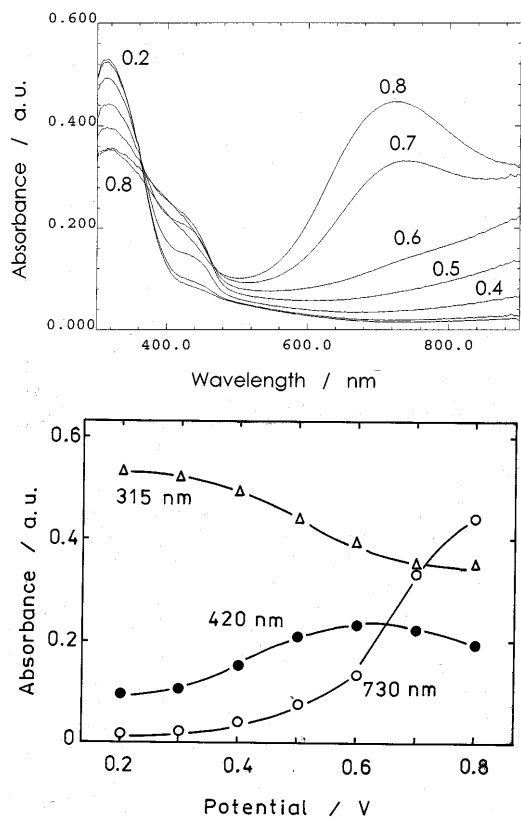dine) form of PNBA. These spectra show an absorbance maximum, located at $\lambda = 315$ nm. In analogy with PANI [17, 18] and some of its ring-substituted derivatives [19], this maximum can be ascribed to the $\pi \mapsto \pi^*$ transition of the benzoid ring in the leucoemeraldine form of PNBA.

By stepping the electrode potential to higher values the growth of absorbance in the red region of the spec-

Fig. 5 *Top*: UV-Vis spectra of a poly(*N*-benzylaniline) (PNBA) modified electrode prepared by electropolymerisation at $E_{RHE} = +1.1$ V in a supporting electrolyte solution at various electrode potential values ranging from $E_{RHE} = +0.2$ to $+0.8$ V, recorded at every 0.1 V (as indicated). *Bottom*: absorbance vs. electrode potential profiles, obtained from spectra as on top for three characteristic absorbance bands located at $\lambda = 315$, $\lambda = 420$ and $\lambda = 730$ nm

trum (beyond $\lambda = 600$ nm) becomes more evident. At $E_{RHE} = 0.7$ or 0.8 V an absorbance maximum located at ca. $\lambda = 720$–730 nm appears [Fig. 5 (top)]. This main absorbance band corresponds to the oxidised (emeraldine) state of PNBA. The growth of absorbance in the red region, proceeding simultaneously with a decrease of the band at $\lambda = 315$ nm by shifting of the electrode potential to higher values, corresponds to the progressive oxidation of PNBA from its leucoemeraldine form, containing benzoid rings, into its emeraldine form, containing conjugated quinoid rings.

Figure 5 (bottom) shows the dependence of absorbance, recorded at three selected wavelengths, on the applied electrode potential. An increase of absorbance at $\lambda = 730$ nm, proceeding simultaneously with a decrease at $\lambda = 315$ nm, take place during a positive potential shift. When recorded at $\lambda = 400$–440 nm the absorbance vs. electrode potential plots show a maximum [Fig. 5 (bottom)]. For PANI films the absorbance band in this region corresponds to non-conjugated quinoid rings [17, 20, 21] formed during partial electrooxidation of the PANI film. As compared to PANI, the maximum position of this transition band of PNBA appears shifted by ca. 0.2 V (i.e., from $E_{RHE} = 0.4$ V

for PANI to 0.6 V for PNBA) to higher potential values. For A,t profiles, obtained at $\lambda = 315$ nm and $\lambda = 730$ nm, the $A^{1/2}$ values are also shifted by 0.1 and 0.25 V, respectively, towards higher potential values, as compared to PANI. These observations are in agreement with the known redox potential shift of the leucoemeraldine to emeraldine transition, characteristic for N-substituted PANI derivatives, as compared to PANI [2].

Figure 6 shows absorbance transients recorded at the same three characteristic wavelengths as in Fig. 5 (bottom) obtained after negative- and positive-going potential steps. After applying an electrode potential of $E_{RHE} = +0.2$ V to the ITO electrode covered with a PNBA layer and held initially at $E_{RHE} = +0.8$ V, a fast decrease of the absorbance at $\lambda = 730$ nm proceeds. After a few or a few tens of seconds the absorbance reaches its minimum value, which does not change for a long time provided that the electrode is held at a constant potential value. Simultaneously, an increase of the absorbance at $\lambda = 315$ nm is observed, reaching a maximum value after a few or few tens of seconds (Fig. 6). At the same time, the absorbance at $\lambda = 420$ nm increases and reaches its maximum value in a short time, and then decreases again to a certain minimum value, characteristic for the reduced form of

PNBA (Fig. 6). After the back positive-going potential step to $E_{RHE} = +0.8$ V the changes of absorbance for the bands located at $\lambda = 315$ nm and $\lambda = 730$ nm proceed in opposite directions (Fig. 6). Also, a maximum on A,t curves for the band at $\lambda = 420$ nm is obtained after a positive-going step, which, however, appears less sharp, as the PNBA film change after a positive potential step proceeds slower, than after the negative one. The same can be concluded by comparing the rate of absorbance growth or decrease for the main absorbance band in the red region of the spectrum obtained after a positive- or a negative-going potential step, respectively. It is seen in Fig. 6 that an increase of the absorbance at $\lambda = 730$ nm, obtained after a positive-going potential step, proceeds slower than the decrease observed after a negative potential step. For all PNBA films investigated, which differ in their thickness [as in Fig. 6 (top) and (bottom)], the ratio of the rate of decrease of absorbance when going to negative potentials to that of the increase of absorbance when going to positive potentials, as recorded at $\lambda = 730$ nm, was found to be ca. 5.1. This means that colouration of a PNBA film after a positive potential step proceeds slower than its discolouration (bleaching) after a negative-going step. This is in agreement with the reported observation that the reductive conversion of PANI films occurs more rapidly than the oxidative conversion [22–24]. For thicker films of PNBA, both the decrease and increase of absorbance for bands at $\lambda = 315$ nm and $\lambda = 730$ nm occur relatively slower than for thinner films [cf. Fig. 6 (top) and (bottom)]. Also, the maxima on A,t dependencies for the band at $\lambda = 420$ nm appear more flattened for thicker films of PNBA.
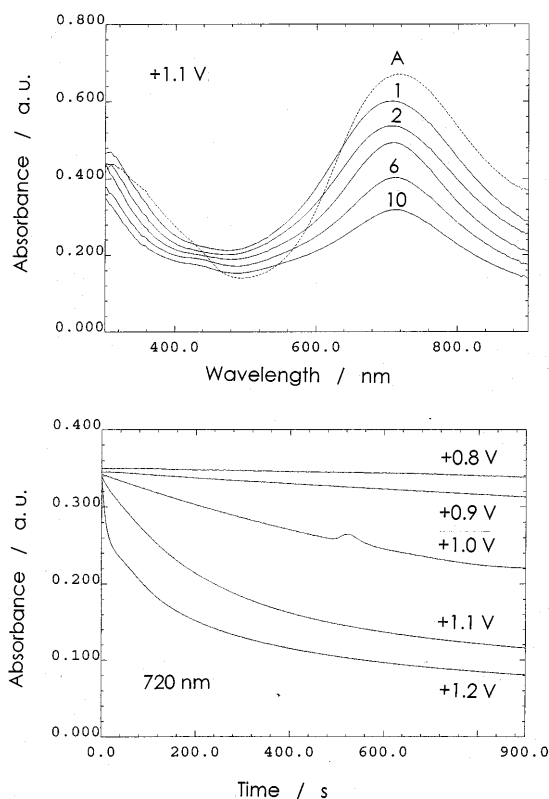
Anodic degradation of PNBA films

The anodic decomposition of conducting polymer films is a well known and documented phenomenon [25–27]. Figure 7 (top) shows UV-vis spectra of PNBA films obtained by holding the electrode at a relatively high positive potential. The decrease of absorbance that was observed in the entire spectral range investigated when holding the PNBA-modified electrode at $E_{RHE} = +1.1$ V indicates an irreversible degradation of the polymer film. The degradation rate depends strongly on the applied electrode potential being higher for a higher positive potential. Figure 7 (bottom) shows kinetic curves recorded at $\lambda = 720$ nm by applying different electrode potential values ranging from $E_{RHE} = +0.8$ V to $E_{RHE} = +1.2$ V. Below $E_{RHE} = +0.8$ V, the degradation proceeds slowly and a PNBA film can be considered as being relatively stable for at least several tens of minutes.

The data of Fig. 7 can be linearised in the first-order reaction coordinates (i.e., ln A vs. t). From the slope of the linearised data a first-order degradation rate constant can be obtained. The corresponding data are collected in Table 1. The first-order rate constants vary

Fig. 6 Change of absorbance for an ITO glass electrode modified with a thin (*top*) and thick (*bottom*) film of PNBA obtained after a potential step to $E_{RHE} = +0.2$ V and $+0.8$ V (as indicated by *arrows*) in monomer-free solution of 0.5 M H_2SO_4, at wavelengths of $\lambda = 730$ nm (*1*), $\lambda = 420$ nm (*2*) and $\lambda = 315$ nm (*3*). Before measurements, electrodes were held at $E_{RHE} = +0.8$ V for 2 min

Fig. 8 Dependence of logarithm of the first-order rate constant for the electrochemical degradation of PNBA (open circles) and polyaniline (filled circles) on electrode potential in a monomer-free supporting electrolyte solution
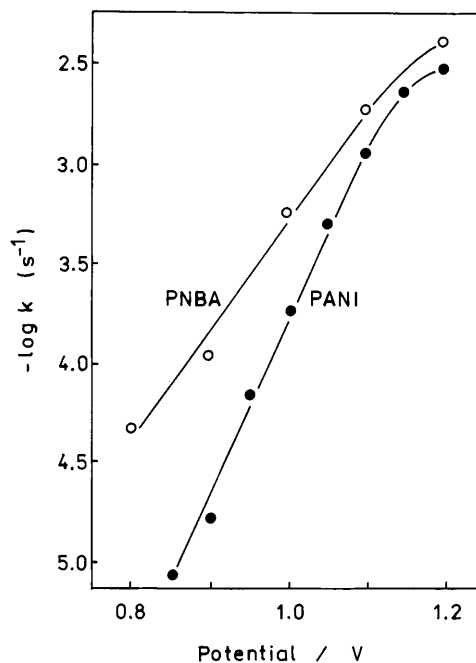
Fig. 7 *Top*: UV-Vis spectrum of a PNBA modified electrode in a supporting electrolyte solution at $E_{RHE} = +0.8$ V (*dashed trace*, indicated by *A*), and spectra, obtained after different time intervals (as indicated, in minutes) after stepping the electrode potential to $E_{RHE} = +1.1$ V. *Bottom*: absorbance-time profiles recorded at $\lambda = 720$ nm, obtained after a potential step to different values (as indicated) for a PNBA coated electrode obtained in supporting electrolyte solution

Table 1 Kinetic parameters for PNBA film degradation, obtained at electrode potentials ranging from $E_{RHE} = +0.8$ to $+1.2$ V

E (V)	k (s^{-1})	$\tau_{1/2}$ (min)	k/k_{PANI}[a]
0.8	4.80×10^{-5}	241 (4.01 h)	16.3
0.9	1.10×10^{-4}	105 (1.75 h)	7.86
1.0	5.50×10^{-4}	21	3.02
1.1	1.84×10^{-3}	6.3	1.64
1.2	3.93×10^{-3}	2.9	1.34

[a] The data on degradation rate constants for polyaniline, used in obtaining the values of k/k_{PANI}, are based on separate experiments not reported here

between 4.80×10^{-5} s^{-1} for an electrode potential of $E_{RHE} = +0.8$ V and 3.93×10^{-3} s^{-1} for the highest potential value tested ($E_{RHE} = +1.2$ V). These values correspond to half-times for polymer film degradation ranging from 4 h for $E_{RHE} = +0.8$ V to 2.9 min for $E_{RHE} = +1.2$ V. For all potential values the degradation of PNBA film proceeds faster than PANI film, especially at lower electrode potentials (Table 1). This indicates a lower stability of PNBA film as compared to PANI based on the results of corresponding experiments not reported here.

The dependence of degradation rate constants on electrode potential can be linearised in the coordinates (log k, E). The data obtained for PNBA films are shown in Fig. 8. For comparison, the corresponding data for PANI films are also shown in Fig. 8 (these data were taken from corresponding experiments not reported here). A linear fit of the data shown can be provided according to the equation:

$$\log k = a + bE$$

where k is a first-order degradation rate constant (expressed in s^{-1}), E is the electrode potential (in V), and a and b are empirical coefficients.

For PNBA films the coefficients $a = -8.75$ and $b = 5.45$ were obtained from a linear fit of the data in the potential range of $E_{RHE} = +0.8$ to $+1.1$ V, with the regression coefficient $r = 0.991$. For PANI, coefficients $a = -12.7$ and $b = 8.96$, with regression coefficient $r = 0.993$, in the potential range of $E_{RHE} = +0.85$ to $+1.1$ V can be obtained. The data show that the degradation of PNBA film proceeds faster than that of PANI.

The above purely empirical relationship is derived from results obtained when monitoring the change of optical absorption of the investigated polymer films. The electronic transition has been assigned to quinoid moieties in the polymer, typical of its oxidized form. The decrease of optical absorption indicates a decrease in the number of these systems in the polymer. The applied positive electrode potential incorporated in the suggested equation does not cause this decrease; actually the

electrode potential causes polymer oxidation and consequently an increase of the number of quinoid units. The decrease of the number of quinoid units is instead caused by nucleophilic attack of electrolyte solution constituents, resulting in more or less far reaching changes of the polymer structure with definitively less electronic absorption at the investigated wavelength. A decrease of absorbance with a positive-going electrode potential implies that, despite the accelerated supply of quinoid units, their destruction is becoming even faster. The chemical reaction (nucleophilic attack) has to be faster than the electrochemical step. The acceleration of this chemical reaction at more positive potentials may be caused by the fact that even shorter conjugated quinoid systems, even more prone to nucleophilic attack, are formed. A more careful investigation of shifts in the absorption maximum (which should move to shorter wavelength with shorter conjugation length), not attempted in this investigation, may shed some light on this suggestion. Despite its apparent simplicity and Tafel-like appearance, the further interpretation of the empirically found relationship between the applied electrode potential and the rate of loss of optical absorption will be better explained only with the advent of more information about the details of the chemical steps following the electrooxidation step.

Electrode processes taking place at PNBA modified electrodes

Figure 9 (top) shows A,t profiles obtained with a PNBA-modified ITO glass electrode after stepping the electrode potential from $E_{RHE} = +0.2$ to $+0.8$ V, as recorded at $\lambda = 730$ nm. Measured in a supporting electrolyte solution only, without redox active species, the absorbance increases and reaches its maximum value in some tens of seconds. In an electrolyte solution containing 1,4-hydroquinone (HQ), a fast initial increase of absorbance, observed after the positive-going potential step, is followed by a slow increase [trace 2 in Fig. 9 (top)]. In the latter case the absorbance does not reach the maximum value characteristic for the supporting electrolyte solution without HQ.

The following reaction sequence, taking place in HQ-containing solution, is proposed. After applying a positive-going potential step, the electrooxidation of the PNBA layer to its emeraldine form proceeds. In the next following step, the emeraldine form of PNBA oxidises HQ to 1,4-benzoquinone (BQ). As a consequence of these reactions, a quasi-equilibrium state is established, characterised by a certain ratio of emeraldine and leucoemeraldine forms in the polymer layer. It may be easily calculated from Fig. 9 (top) that at the quasi-equilibrium state an emeraldine fraction of ca. 0.46 is present in the PNBA layer. For comparison, Fig. 9 (bottom) shows A,t profiles, obtained under identical conditions, for a PANI-modified ITO glass electrode. An emeraldine fraction of ca. 0.81, present in the PANI
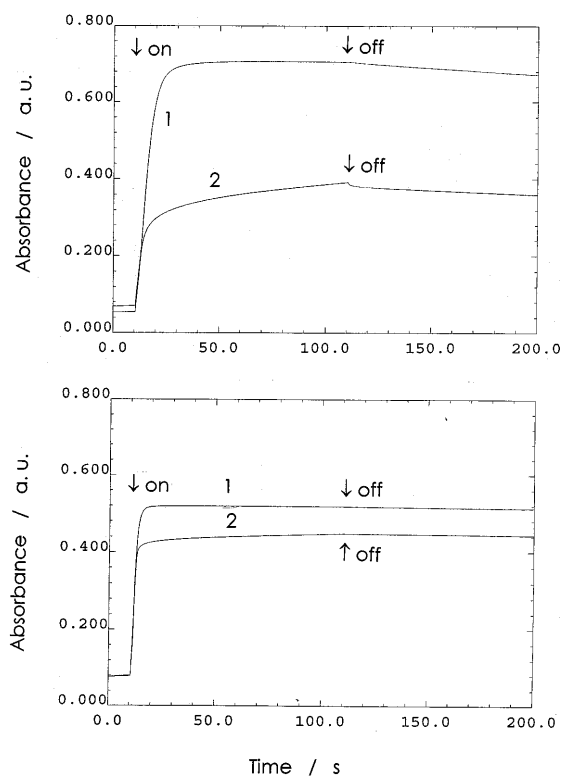
Fig. 9 *Top*: change of absorbance at $\lambda = 730$ nm for an ITO glass electrode modified with a PNBA film after a potential step to $E_{RHE} = +0.8$ V and after interruption of electrolysis (as indicated by *arrows*) in a supporting electrolyte solution (*1*), and in the same solution containing in additional 50 mM of 1,4-hydroquinone (*2*). *Bottom*: same as on top with a polyaniline-modified ITO glass electrode

film at the quasi-equilibrium state, can be obtained from these data. The data obtained show that obviously the anodic oxidation of PANI proceeds more efficiently than of PNBA, leading to a greater content of the oxidised form of the polymer present in the course of the electrooxidation of HQ.

Figure 10 shows A,t profiles obtained after a negative-going potential step with a PNBA modified electrode held initially in its oxidised form at $E_{RHE} = +0.8$ V. A fast decrease of absorbance is observed after stepping the electrode potential to $E_{RHE} = +0.2$ V (trace 1 in Fig. 10). In the presence of BQ the absorbance does not reach its minimum value. Instead, a quasi-equilibrium is established in some tens of seconds, indicating that a part of the polymer is in its oxidised state. This means that electrochemical reduction of PNBA film is followed by its reoxidation with BQ. As a result, a quasi-equilibrium state is established, characterised by a certain ratio of oxidised and reduced forms of PNBA, present in the film. As may be expected, it follows from Fig. 10 (top) that this ratio depends on the BQ concentration in solution. It may be calculated from the data of Fig. 10 (top) that by changing the concentration of BQ from 5 to 20 mM the emeraldine content of PNBA film varies from 0.13 to 0.22, i.e. an increase of
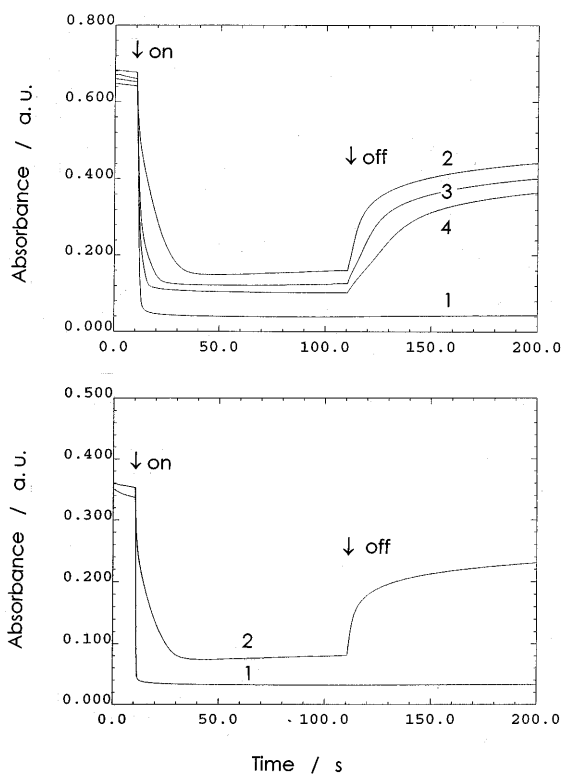
Fig. 10 Change of absorbance at $\lambda = 730$ nm for an ITO glass electrode modified with thick (*top*) and a thin (*bottom*) film of PNBA after a potential step to $E_{RHE} = +0.2$ V and after interruption of electrolysis (as indicated by the *arrows*) in a supporting electrolyte solution (*1*) and in the same solution containing in additional 1,4-benzoquinone in a concentration of 20 mM (*2*), 10 mM (*3*), and 5 mM (*4*). Before experiments the electrode was held at $E_{RHE} = +0.8$ V for 2 min

BQ concentration causes an increase of emeraldine content in the film, obviously because of an enhancement of the chemical oxidation of the film. With thinner PNBA films, a lower content of the oxidised form of polymer is reached at equilibrium under otherwise identical conditions. For example, by comparing the traces of Fig. 10 (top and bottom) it can be calculated that for thicker (top) and thinner (bottom) films, emeraldine contents of 0.22 and 0.17, respectively, are attained at equilibrium, reached with the use of BQ in a concentration of 20 mM. A relative film thickness, used in obtaining the data of Fig. 10 (top and bottom), is ca. 1.0 and 0.8, respectively.

The results obtained show that a PNBA film is able to act as an electron transfer mediator in a coupled electrochemical/chemical redox process with the participation of solute redox species, such as BQ or HQ.

References

1. Chiba K, Ohsaka T, Oyama N (1987) J Electroanal Chem 217: 239
2. Barbero C, Miras MC, Haas O, Kötz R (1991) J Electroanal Chem 310: 437
3. Comisso N, Daolio S, Mengoli G, Salmaso R, Zecchin S, Zotti G (1988) J Electroanal Chem 255: 97
4. Langer JJ (1990) Synth Met 35: 295
5. Langer JJ (1990) Synth Met 35: 301
6. Dao LH, Leclerc M, Guay J, Chevalier JW (1989) Synth Met 29: E377
7. Dao LH, Guay J, Leclerc M (1989) Synth Met 29: E383
8. Malinauskas A, Holze R (1998) Electrochim Acta 43: 521
9. Malinauskas A, Holze R (1998) Electrochim Acta 43: 515
10. Yano J, Kokura M, Ogura K (1994) J Appl Electrochem 24: 1164
11. Malinauskas A, Holze R (1996) Ber Bunsenges Phys Chem 100: 1740
12. Malinauskas A, Holze R (1997) Ber Bunsenges Phys Chem 101: 1859
13. Malinauskas A, Holze R (1998) Electrochim Acta 43: 2413
14. Genies EM, Lapkowski M (1987) J Electroanal Chem 236: 189
15. Shim YB, Won MS, Park SM (1990) J Electrochem Soc 137: 538
16. Chiba K, Ohsaka T, Oyama N (1987) J Electroanal Chem 217: 239
17. Hochfeld A, Kassel R, Schultze JW, Thyssen A (1988) Ber Bunsenges Phys Chem 92: 1406
18. Scully M, Petty MC, Monkman AP (1993) Synth Met 55–57: 183
19. Probst M, Holze R (1996) Ber Bunsenges Phys Chem 100: 1286
20. D'Aprano G, Leclerc M, Zotti G (1993) J Electroanal Chem 351: 145
21. Stilwell DE, Park SM (1989) J Electrochem Soc 136: 427
22. Kalaji K, Peter M, Abrantes LM, Mesquita JC (1989) J Electroanal Chem 274: 289
23. Aoki K, Cao J, Hoshino Y (1993) Electrochim Acta 38: 1711
24. Tezuka Y, Kimura T, Ishii T, Aoki K (1995) J Electroanal Chem 395: 51
25. Kobayashi T, Tamura H, Yoneyama H (1984) J Electroanal Chem 177: 293
26. Horanyi G, Inzelt G (1989) J Electroanal Chem 264: 259
27. Pud AA (1994) Synth Met 66: 1